RSS Based Technologies in Wireless Sensor Networks

Samitha Ekanayake and Pubudu Pathirana
Deakin University
Australia

1. Introduction

Recent advances in electronics, computing and wireless communication technologies have made possible the use of low cost, low power sensor nodes with processing and wireless communication capabilities for variety of monitoring and control applications. A Wireless Sensor Network (WSN) is a collection of densely deployed such sensor nodes, having a collaborative objective. In typical WSN applications the positions of the sensor nodes are not engineered or predetermined. Instead the nodes are randomly deployed into the scenario. For example, in a large environmental monitoring sensor network (lake, forest, or seabed) involving thousands of sensor nodes, the nodes may be air dropped into the area of interest. In such WSN, the nodes are entirely dependent on the limited energy reserves such as batteries. Therefore nodal energy conservation is of utmost importance for prolonged network life. In this chapter we explore some RSS (Received Signal Strength) based techniques for power conservation in such randomly deployed WSN.
Although the WSN concept is being extensively explored in the recent past, there has not been an all-in-one communication scheme which satisfies the requirements of every networking scenario. We consider two networking scenarios which incorporate RSS based transmission power controlling to ensure Quality of Service (QoS) guaranteed communication links and to save limited nodal energy reserves. Both networking scenarios are having high application value in WSN arena, an all-to-all networking scenario and a mobile data collector based data collection network. In both networks we consider wireless nodes with multiple access communication capabilities (such as CDMA).
Among the multiple access schemes in wireless communications, CDMA has become the most promising technology that can satisfy most aspects in modern communication networks, such as higher speeds, larger client base and QoS guaranteed communication. Although CDMA started service in cellular communications in late 90's, the concept was originally introduced by Claude Shannon and Robert Pierce in 1949 (Ellersick 1984), and then extended by DeRosa-Rogoff, Price & Green and Magnuiki (Cooper and Nettleton 1978; Prasad and Ojanpera 1998). The early developments of this technology were primarily focused on the military and navigation applications (Batchelor, Ochieng et al., 1996). As the first civilian application, a narrow-band spread spectrum CDMA scheme for cellular communication was first proposed by Cooper and Nettleton in 1978 (Scholtz 1994) and then

developed to the IS-95 and CDMA2000 standards which are used in modern CDMA wireless communications (Knisely, Kumar et al. 1998).

Maintaining the Carrier-to-Interference Ratio (CIR), alternatively referred as the co-channel interference, at a desirable level is the main aspect of power control in CDMA networks. In CIR balancing, the transmission powers of every user device is controlled such that it ensures the co-channel interference of each link guarantees QoS reception. CIR balancing in a cellular system has two aspects: intra-cell CIR balancing and inter-cell CIR balancing. In intra-cell CIR balancing the user devices control the transmission power such that it provides a constant received power at the base station (Gilhousen, Jacobs et al. 1991) to avoid near-far problem. This method is currently in practice with CDMA standards such as IS-95 and CDMA 2000 (Schiller 2003). Inter-cell CIR balancing received widespread attention among the academic community after the problem reformulation by Zander et al. in (Zander 1992). This work was further investigated by Grandhi et al. (Grandhi, Vijayan et al. 1993; Grandhi, Vijayan et al. 1994; Grandhi, Yates et al. 1997) and the Distributed Power Control (DPC) scheme proposed by Foschini and Miljanic (Foschini and Miljanic 1993) has become a standard benchmark due to its academic and practical significance (see (Cai, Wang et al. 2004; Uykan and Koivo 2004; Uykan and Koivo 2006) for further improvements), which was later adopted into wireless communication standards.

Wireless sensor networks are inherently associated with restrictions in power consumption mainly due to the limited energy resources such as batteries. Therefore, unlike in cellular communications, the power control in wireless ad-hoc networks are basically focused on energy conservation. Many power conservation techniques introduced for such networks can be found in the past research literature (ElBatt and Ephremides 2004; Lim, Leong et al. 2005; Hou, Shi et al. 2006; Klein and Viswanathan 2006; Gomez and Campbell 2007). Among them routing optimization (ElBatt and Ephremides 2004; Hou, Shi et al. 2006; Klein and Viswanathan 2006) and transmission power control (Gomez and Campbell 2007) are the widely researched areas. However as opposed to the above, different effective methods such as sleep and wakeup procedures implemented in the hardware layer (Lim, Leong et al. 2005), were also proposed.

In the next section we discuss an all-to-all network for a wireless sensor network having multiple access communication capabilities. Such communication scheme is benificial for sharing of sensor data within the sensor network for real-time processing and decision making. The power control algorithm enable every node in the network to communicate with each other at the same time while consuming the minimum amount of energy for communication. In section 3, we introduce a transmission power control algorithm for a WSN having a mobile data collector based data gathering system. This scheme ensures maximum communication duration for nodes and the mobile data collector while using minimum possible energy for data communication.

2. All-to-all networking for instantaneous data sharing among the nodes

Recent past has witnessed a growing popularity in the multi-cast networking technologies, which have added advantages in the modern communication needs such as internet based multimedia services (news, distant learning etc), multimedia conferencing facilities for computers and mobile phones (Almeroth 2000; Chan, Modestino et al. 2007).

In multi-casting, the broadcasting of a single data packet to the network by the node dramatically improves the bandwidth usage in comparison to the unicast networks (one-to-one networks). In addition to the multimedia communication; distributed computing, parallel processing , swarm robotics , and wireless sensor networks where each node have some information to share with the other nodes have distinct advantages in employing all-to-all networks (multi-casting) (Chen, Chen et al. 1996).

All-to-all communications, proposed by Yang and Wang can be classified as: all-to-all broadcasting and all-to-all personalized exchange depending on the nature of the communication (Yang and Wang 2001). In the former case, the information (data packet) originating from a single node is propagated through the entire network and in the latter case every node has distinct information to share with every other node in the network. Routing algorithms for both network types have been extensively researched in the past (Akyildiz, Ekici et al. 2003; Guo and Yang 2006; Transier, Fubler et al. 2007). However, these routing algorithms were based on multi-hopping mesh and torus based network architectures and involve routing tree generation, forwarding link assignments, sub-network creation etc. They also have many practical difficulties in applying to all-to-all ad-hoc networks (Yang and Wang 1998; Yang 2006). In modern distributed / parallel processing applications, the network essentially consists of time varying nodes (location changes and addition / removal of nodes), which cause changes in the mesh / torus at each instance of architectural change. Moreover, those multi-hopping all-to-all networks comprises of hopping (routing) delays and increased network congestion with increasing network traffic, resulting in loss of vital information.

In this discussion, we consider a situation where an ad-hoc connected multiple-node wireless network requiring instantaneous all-to-all personalized communication, which is distributed within a close range such that the single-hop communication can be achieved between every node. The communication scheme introduced here enables all-to-all networking of the nodes without forwarding tree generation based on the spatial configuration of the nodes, i.e. node mobility, addition / removal of nodes etc. The proposed network uses CDMA based communication architecture which enables the entire network to communicate simultaneously. Moreover, we derive the capacity of the network in-terms of the number of nodes in the network and introduce a power control algorithm which ensures that all the nodes are transmitting at the minimum possible transmission power while maintaining the connectivity of the entire network ensuring interference free communication.

2.2 Problem Formulation

Now we formally introduce the power control problem together with the associated network architecture, control constraints and network capacity.

(a) Network Architecture:

Consider a single hop all-to-all wireless network (Ω) in which N nodes communicate with each other simultaneously (see Fig 1) using spread-spectrum multiple access protocol (such as CDMA). In this network, the nodes are broadcasting the data continuously, rather than maintaining node-to-node communication links. The broadcast data from a particular node, which is uniquely coded, can be accessed by every other node in the network.

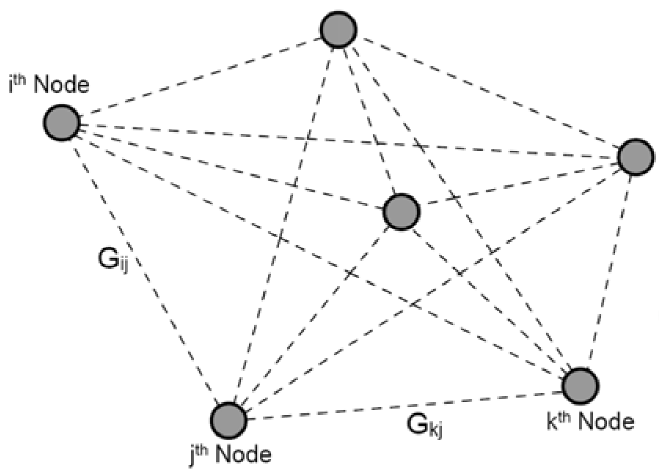

Fig. 1. - An all-to-all network consisting of six nodes.

The network model assumes followings;

- Nodes have instantaneous and error free Received Signal Strength (RSS) measurement capabilities.
- The measurements are immediately included in to the broadcast data, which will be used for the PC process.
- Link gain variations are negligible compared with the communication and the data processing time.
- All the nodes in the network are identical in performance (homogeneous).

In the controller analysis, the above assumptions are used in order to reduce the system complexity; however in later sections we relax these assumptions and present the controller behavior with erroneous measurements, non-homogeneous node properties, and link gain variations which resemble a real-world scenario.

(b) Control Constraints:

In order to achieve QoS guaranteed communication in every link, two conditions must be satisfied simultaneously; CIR constraint and the connectivity constraint.

CIR Constraint : Any node j in the network can receive the signal transmitted from any other node i, correctly, if the CIR measured at the j^{th} node (γ_{ij}) is greater than the threshold CIR value γ_t. Then the CIR constraint can be defined as;

$$\gamma_{ij} = \frac{P_i G_{ij}}{\sum_{k \neq i, k \neq j}^{N} P_k G_{kj} + \eta} \geq \gamma_t, \forall i, k, j \in \Omega \quad (1)$$

where P_i is the transmission power levels of the i^{th} node. In the above expression, G_{ij} and G_{kj} are the link gains between i, j and k, j nodes respectively. Here the η represents the noise power (thermal noise) in the communication link and this is assumed to be constant for the geographical area (see (Foschini and Miljanic 1993; Uykan and Koivo 2004)).

Connectivity Constraint: To receive a signal from any node i, the received power level of the signal measured at the j^{th} node (R_{ij}) must be greater than the receiver threshold R_{min}, which is the sensitivity of the receiver hardware. In this study the threshold received power is defined such that, the reception is not affected by the thermal noise of the band. Then the received power condition can be defined as (considering $R_{ij} = P_i G_{ij} + \eta$);

$$P_i G_{ij} + \eta \geq R_{min}, \forall i,, j \in \Omega. \tag{2}$$

(c) Capacity and spatial limitations:
In order to satisfy the above constraints, the all-to-all network has certain limitations in the spatial configuration and network capacity. This section derives the network capacity which ensure QoS guaranteed communication, and the relationships between the receiver sensitivity and the spatial configuration (link gains) to maintain reliable links.
From the connectivity constraint we get,

$$\min_{i,j\in\Omega}\left(P_i G_{ij} + \eta\right) \geq R_{min}, \tag{3}$$

which provides a condition that the network should satisfy at all the times for the power control algorithm to perform the desired action. Moreover, the network always satisfies the connectivity constraint (``*connectivity guaranteed*'' networks) if:

$$P_{min} G_{min} \geq R_{min} - \eta; \tag{4}$$

and the network is ``*feasible*'' if:

$$P_{max} G_{min} \geq R_{min} - \eta. \tag{5}$$

Here, P_{min} and P_{max} refers to the minimum and maximum transmission power levels of the nodes respectively, and G_{min} is the minimum link gain between any two nodes in the network. Above, the term ``*feasible*'' means that the network can achieve the connectivity constraint.

From the CIR constraint (equation (1));

$$\min_{i,j\in\Omega}\left(P_i G_{ij}\right)\left(\frac{1+\gamma_t}{\gamma_t}\right) \geq \max_{k,j\in\Omega}\left(\sum_{k\neq j}^{N} P_k G_{kj} + \eta\right), \tag{6}$$

thus for ``*connectivity guaranteed*'' network:

$$P_{min} G_{min}\left(\frac{1+\gamma_t}{\gamma_t}\right) \geq (N-1) P_{max} G_{max} + \eta,$$

resulting,

$$N \leq 1 + \left(\frac{1+\gamma_t}{\gamma_t}\right)\left(\frac{P_{min} G_{min}}{P_{max} G_{max}}\right) - \left(\frac{\eta}{P_{max} G_{max}}\right). \tag{7}$$

For the ``*feasible*'' network:

$$P_{max} G_{min}\left(\frac{1+\gamma_t}{\gamma_t}\right) \geq (N-1) P_{max} G_{max} + \eta,$$

limiting the capacity as,

$$N \leq 1 + \left(\frac{1+\gamma_t}{\gamma_t}\right)\left(\frac{G_{min}}{G_{max}}\right) - \left(\frac{\eta}{P_{max} G_{max}}\right). \tag{8}$$

Definition 1. Limited Capacity Network: A multi-casting network satisfying the equation (8) on the number of nodes is defined as a Limited Capacity Network.
Remark: In above derivations, the network capacity is determined in terms of the number of nodes connected (N) at an instance and this number is dependent on the target CIR (γ_t). In spread spectrum networks, γ_t is selected to maintain the desired network quality, bandwidth and the data transfer speed (Gilhousen, Jacobs et al. 1991). Thus limiting the number of nodes to N ensures that the desired communication capacities/qualities are preserved in the network.
Remark: In limited capacity networks, the range of link gains in the desired geographical area ($G_{ij} \in [G_{min}, G_{max}]$) is a decisive factor on the number of nodes. However, this enables us to accurately select the number of nodes to be deployed in a particular region, knowing the range of link gain at that region.
Remark: In limited capacity networks, the maximum number of nodes (N_{max}) is defined such that the networks always satisfy the CIR constraints without directly depending on the spatial distribution of the nodes. However, this does not mean that a network with number of nodes $N > N_{max}$ in the same geographical area (not necessarily in the same configuration) does not satisfy the CIR constraints.

(d) Intended Controller Behavior for Energy Conservation:
In this power control problem, we consider an ad-hoc network satisfying ``*Limited Capacity*'' and "*feasible*" conditions. The problem considered here is to maintain all-to-all communication links in such networks, while minimizing the network power consumption via transmission power control. The proposed power control algorithm is focused on maintaining minimum requirements for satisfying the connectivity constraints, which automatically satisfies the CIR constraint in a Limited Capacity network.

2.3 Iterative Controller

In this section, we present a transmission power control scheme (see Fig 2) to maintain the received powers at the desired value that satisfy the connectivity of the network, and derive the tolerance limit for selecting the target received power.
The transmission power of the i^{th} node (P_i) is determined by,

$$\dot{P}_i = a(e_i - R_t), \tag{9}$$

here $a < 0$ is a constant, e_i is the average received power at the other nodes, i.e $e_i = \frac{\sum_{j \neq i}^{N} \left(P_i G_{ij} + \eta\right)}{N-1}$, and R_t is the target received power which satisfy the connectivity constraint for all the nodes. In this power control algorithm, we assume that the nodes are transmitting at the maximum transmission power at time zero (at the initialization of the algorithm).

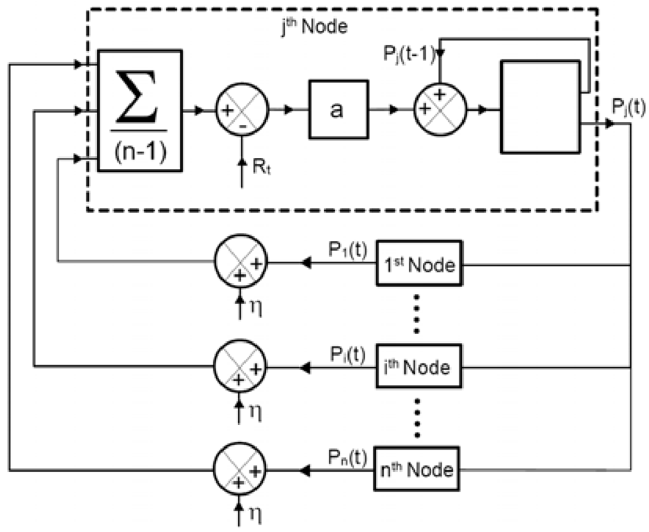

Fig. 2. - Block diagram representation of the controller of the j^{th} node

(a) Convergence of the controller

From the definition we have, $e_i = P_i A_i + \eta$ and thus $\dot{e}_i = \dot{P}_i A_i$, where $A_i = \frac{\sum_{j \neq i}^{N} G_{ij}}{N-1}$ is the ``average link gain'' for the i^{th} node.

With this, the controller function can be reformulated as:

$$\dot{e}_i = aA_i(e_i - R_t),$$

From the above expression it is evident that the control variable e_i converges to R_t, if $\| aA_i \| < 1$. Since $G_{i,j} < 0, \forall i, j$ and selecting $\| a \| < 1$ always satisfies the $\| aA_i \| < 1$ condition for the convergence.

(b) Satisfying Connectivity for Every Node

The convergence of the above controller describes the trajectory of the average received power, however, it does not say anything about the trajectories of the RSS in each link or their connectivity. In this section, we obtain a relationship between link gains, sensitivity of the receiver hardware and the target RSS value, which can be used to determine the tolerance limit when selecting R_t. This relationship is formally introduced in the following proposition.

Proposition 1: In an all-to-all network using the power controller described by (9) and deployed in a geographical area having link gains within a known range, i.e. $G_{ij} \in [G_{min}, G_{max}]$, the connectivity constraint is always satisfied if the threshold value for the power controller, $R_t \geq \frac{R_m + \eta(X-1)}{X}$, where $X = \min_{i,j \in \Omega}\left(\frac{G_{ij}}{A_i}\right)$.

Proof. Let the error between the average RSS and the RSS of the node j,

$$e_{ij} = R_{ij} - e_i = P_i\left(G_{ij} - A_i\right)$$

and the time derivative;

$$\dot{e}_{ij} = \dot{P}_i\left(G_{ij} - A_i\right).$$

Then using the control function (9) we have,

$$\dot{e}_{ij} = aA_i\left[e_{ij} - (R_t - \eta)\left(\frac{G_{ij}}{A_i} - 1\right)\right]. \tag{10}$$

Above expression implies that e_{ij} converges toward $(R_t - \eta)\left(\frac{G_{ij}}{A_i} - 1\right)$, if the conditions for the convergence of e_i are satisfied. Since the above statement is valid for any node i, j in the network, we can determine the lower bound of e_{ij} as;

$$\min_{i,j\in\Omega}(e_{ij}) \le (R_t - \eta)\left(\min_{i,j\in\Omega}\left(\frac{G_{ij}}{A_i}\right) - 1\right). \tag{11}$$

For an all-to-all ad-hoc network deployed in the geographical area with $G_{ij} \in [G_{min}, G_{max}]$, we have;

$$\min_{i,j\in\Omega}\left(\frac{G_{ij}}{A_i}\right) = \frac{(N-1)G_{min}}{G_{min} + (N-2)G_{max}}. \tag{12}$$

Then, the connectivity condition for any link i, j is satisfied if,

$$R_t + \min_{i,j\in\Omega}(e_{ij}) \ge R_{min},$$

i.e.

$$R_t \ge \frac{R_m + \eta(X-1)}{X} \tag{13}$$

where,

$$X = \min_{i,j\in\Omega}\left(\frac{G_{ij}}{A_i}\right)$$

which proves the assertion.

2.4 Simulation Results

(a) Power control algorithm: In this section a simulation case study is presented which illustrates the behavior of the system in an ideal situation described in the problem formulation section. The following parameters were selected for the simulation, $P_i \in [0.1, 3], G_{ij} \in [0.3, 0.6], R_{min} = 0.1, \gamma_{min} = 0.1$, $\eta = 0.05$, and $N = 4$.

With the selected parameters, the *feasible* condition ($R_{min} \le 0.3 \times 3 = 0.9$) and the ``Limited Capacity'' network condition $\left(N \le 1 + \left(\frac{1.1}{0.1}\right)\left(\frac{0.3}{0.6}\right) - \frac{0.05}{0.6} = 6.417\right)$ are satisfied. The target received power (R_t) is selected using equation (13) as: $R_t = 0.2 > \frac{0.1+0.05(0.6-1)}{0.6} = 0.1333$. The simulation results are shown in Fig 3. It is evident from the simulation figures that the controller converges to the minimum transmission power that satisfies all the constraints described in the previous section.

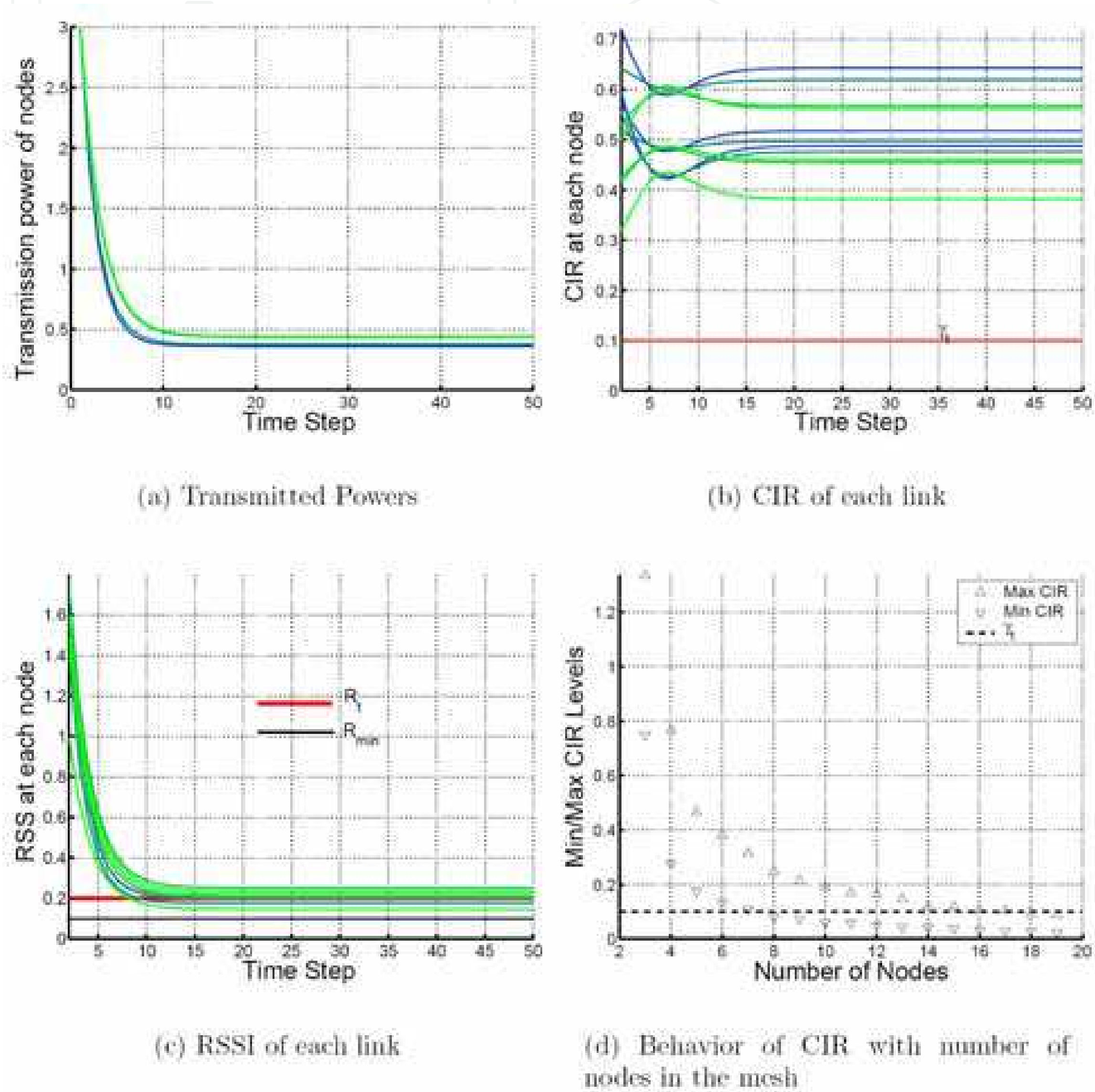

(a) Transmitted Powers

(b) CIR of each link

(c) RSSI of each link

(d) Behavior of CIR with number of nodes in the mesh

Fig. 3. - Effect of the transmission power control algorithm

(b) Network limitations: In this section we evaluate the theoretical assertions on the network limitations. In Fig 3.(d), the variation of CIR with increasing number of nodes is presented. In this figure, minimum and maximum CIR values for each node count are obtained by executing the simulation for 20 times with random selection of gain matrix , $G_{ij} \in [0.3,0.6]$ and all other values are kept as in the previous case. It can be seen that the CIR range drops below the threshold value of 0.1 just after the node count exceeds 7 (the calculated maximum node count $N < 6.417$).

(c) Controller behavior in a real-world scenario: In this section, we illustrate the behavior of the proposed control scheme in the presence of real-world communication properties. Here the network is considered to have hertogeneous nodes, erroneous measurements and link gain variations (due to motion and other mobile obstacles).

The measurement error at j^{th} node is modeled as a normal distribution $\nu_j \in [0,\sigma_\nu^2]$, and the link gain is modelled as $\hat{G}_{ij} = G_{ij}10^{(X/10)}$, where X is the dB attenuation due to shadowing effect and modelled as a Gaussian variable in the form of $X\ N(0,\sigma_X^2)$. Then the received power measurement can be modeled as,

$$R_{ij} = \left(P_i\hat{G}_{ij} + \eta\right)10^{\nu_j/10}. \tag{14}$$

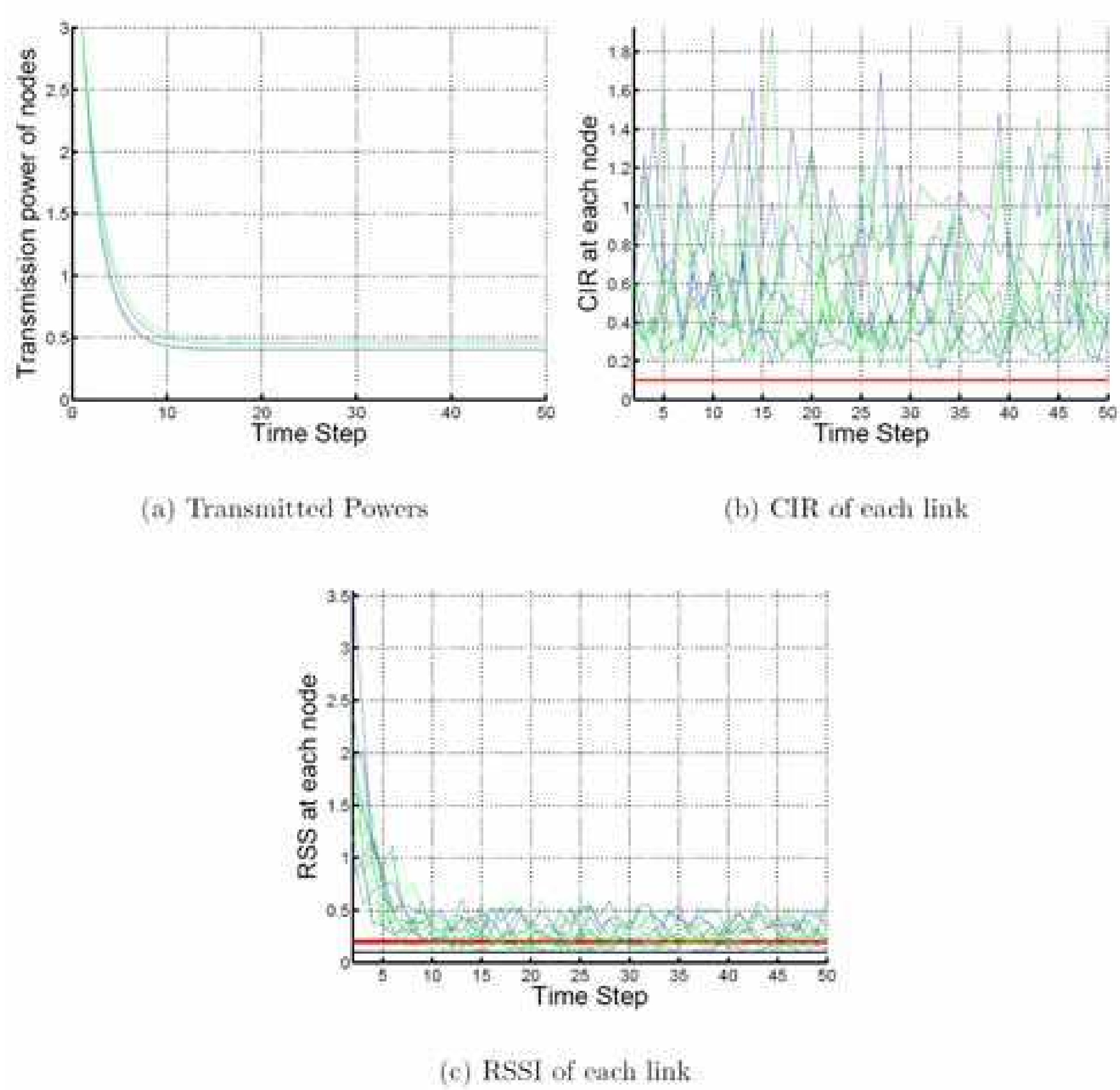

(a) Transmitted Powers

(b) CIR of each link

(c) RSSI of each link

Fig. 4. - Effect of the transmission power control algorithm - Real world scenario

The hetrageneous properties are modelled as differences in power transmission and power measurements, which are common in real-world communication equipments. The actual transmission power of the i^{th} node is modelled as $\hat{P}_i = \alpha_i P_i$, where $\alpha_i \in (\alpha_{min}, 1)$ determines the power of the transmitter and is unique to each node. Similarly, the received power measurement performance factor $\beta_i \in (\beta_{min}, 1)$ determines the actual measured received power $\hat{R}_{ij} = \beta_i R_{ij}$.

In the simulation results shown in Fig 4, we consider $\sigma_X = 2$, $\sigma_v = 0.4$, $\alpha_{min} = 0.8$ and $\beta_{min} = 0.7$ (α_i and β_i values are randomly assigned for each node). According to the simulation results, the power control algorithm performs well in the presence of real-world limitations, maintaining the CIR of every link above the target (threshold CIR) as well as RSS of every link above the minimum RSS.

3. A simple power control algorithm for mobile data collector based remote data gathering scenario

In most low end networking devices CIR can not be directly measured, instead received power (in dBm) and Link Quality measurements can be obtained directly from the hardware. This raise the need of power control algorithms which do not entirely depending on CIR measurements, but depends on rather measurable parameters. In this study we derive the optimum value for co-channel interference measured at a base station, and introduce two power control algorithms to implement in user devices which can alter the transmission power to obtain the required CIR. In the proposed schemes we make use of Received Signal Strength (RSS) measurements to achieve the desired CIR at the base station.

3.1 Problem formulation

In this section we introduce the basic assumptions and models which will be used in the power control scheme. In this study we use the term ``Server'' to denote the base station node which communicate with all the ``Clients'' within the range. Here ``Client'' refers to the sensory node/ user device which is connected to the base station. The following notation is used throughout the paper.

P_i^T	Transmission power of i^{th} node. (dBm)
P_m^T	Transmission power of server node. (dBm)
R_i^m	Received power measured at client i, transmitted by server node. (dBm)
R_m^i	Received power measured at server node, transmitted by node i. (dBm)
R_0^m	Received power measured at reference distance (d_0), transmitted by server node. (dBm)
R_0^i	Received power measured at reference distance (d_0), transmitted by client node i. (dBm)

Consider a wireless network with n clients connected to a single base station in a typical environment consisting of uncertainties in RF propagation due to shadowing, multi path propagation etc. The clients communicate with the server continuously using a common frequency band (as in CDMA). The server has a limit of n_{max} clients connected with it at an instant, and has a receive threshold of R_{min} (dBm) which is depending on the sensitivity of the receiver hardware. Also we assume that the communication network is not interfered by any other RF network in the domain of the base station (or ``cell'' in the cellular networking terminology). Throughout this paper, we assume that the server and the client maintain a continuous communication link, in which the server sends an acknowledgment signal back to the client for each data packet received (similar to (Uykan and Koivo 2004)). This signal contains the RSS of the received packet and the transmission power (if not transmitting at a fixed power) of the acknowledgment signal, which will be used in the PC algorithm. Also the communication hardware (server and client) have the capability to measure the RSS of each data packet.

3.2 Path loss model

We use the following path loss models for communication between the client node and the server node,

$$R_m^i = R_0^i - 10\eta log_{10}\left(\frac{d}{d_0}\right) + S_{im} \tag{15}$$

and

$$R_i^m = R_0^m - 10\eta log_{10}\left(\frac{d}{d_0}\right) + S_{mi}\ , \tag{16}$$

here term η refers to the path attenuation factor, which is a constant depending on the propagation media. In above expressions, S_{im} and S_{mi} refer to the combined effects due to shadow fading, multi-path propagation and any other fading effect occur from environmental factors such as presence of people, animals etc.

For line-of-sight communication in outdoor environments, specially long distance, the propagation of RF (Radio Frequency) waves can be approximated using free-space path loss model. This is possible as multi-path propagation and shadow fading effects do not become significant in such environments. Whereas, for wireless networks in indoor environments, the propagation is harder to predict due to presence of multi-path effects. Many researchers have studied the phenomenon of multi path propagation and proposed RSS models for indoor environments with the presence of obstacles (Tam and Tran 1995; Erceg, Greenstein et al. 1999; Santos, Alvarez et al. 2005; Sato, Sato et al. 2005; Puccinelli and Haenggi 2006). Applicability of those models for mobile nodes is debatable due to dynamic nature of environments and thus the model. Further, the experimental studies done by Lin et. al. in (Lin, Zhang et al. 2006) claims that the RSS value between two nodes in the line of sight have significant changes over the course of the day, thus location based mathematical models become inapplicable.

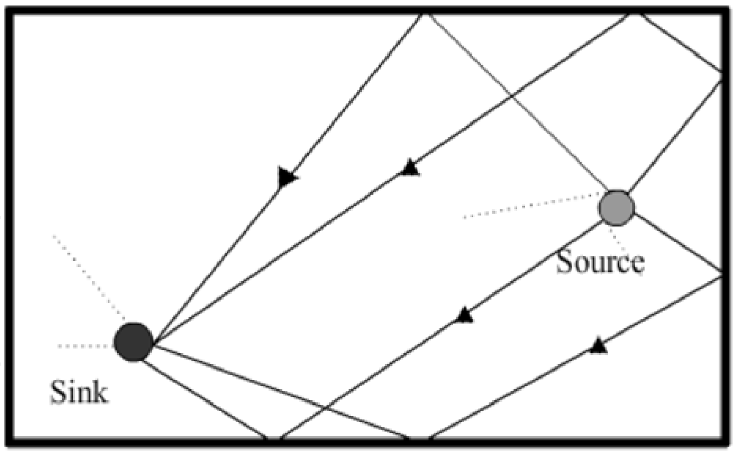

Fig. 5. - Modeling of 2D Multi-path propagation inside an enclosed environment, the figure presents few possible paths of multi-path propagation.

Ray-tracing concept for RF propagation, on the other hand, become a handy tool for predicting RSS variation in an indoor environment (Agelet, Fontan et al. 1997; Degli-Esposti, Lombardi et al. 1998; Remley, Anderson et al. 2000). Here, the radio waves are considered to follow the properties similar to visual light propagation in the presence of transparent obstacles. The effectiveness of Ray-Tracing method for RF waves increases with high frequencies. This is due to reduced scattering effects in shorter wave lengths. We use ray-tracing concept to make an assumption on the S_{xx} terms in equation (15) and (16), as follows;

$$S_{mi}(k) = S_{im}(k), \forall i = 1..n$$

where k represents a time step in discrete time.
As in Fig 5, there exists more than one path for receiving the signal from a RF source to a sink, and the overall S_{xx} term consists combination of all the multi-path propagation terms. With the assumption above, we claim that if the sink and source positions in the Fig 5 was interchanged then the only difference with the previous case is that the direction of propagation. That is all the multi-path links remain the same except the direction, thus results the same S_{xx} effect at the sink in the new configuration. The following experimental results justifies our assumption.

Basis for Ray-Tracing Assumption: In this experiment, four nodes (stationary nodes) were placed in an indoor environment and a mobile node communicating with them was randomly moved in the same environment. The received powers at each stationary node and the received power of the corresponding acknowledgment signal at mobile node were recorded. All the nodes are transmitted in a fixed transmission power and the corresponding R_0^m and R_0^i values were measured with $d_0 = 10cm$ (this was conducted in a large open space to minimize the effect of multi-path propagation). Then the expected value of the $S_{im} - S_{mi}$ can be written as follows.

$$E(S_{im} - S_{mi}) = E(R_m^i) - E(R_i^m) + E(R_0^m) - E(R_0^i)$$

The statistical data of the measurements and calculated $S_{im} - S_{mi}$ are presented in Table 1.

Parameter	Node 1	Node 2	Node 3	Node 4	Node 5
$E(R_m^i)/(dBm)$	-62.56	-65.96	-62.20	-62	-64.01
$E(R_i^m)/(dBm)$	-62.00	-64.00	-61.99	-61.94	-66.00
$E(R_0^i)/(dBm)$	-39.28	-40.65	-39.00	-41.00	-37.01
$E(R_0^m)/(dBm)$	-39.00	-39.00	-38.08	-41.00	-39.00
$E(S_{im} - S_{mi})/(dBm)$	0.29	0.31	-0.72	0.06	0.00

Table 1. - Expected values of measurements

From the experimental data it is evident that the $S_{im} - S_{mi}$ term is zero. In this experiment, even though all the transmitters are transmitting with the same power, we used the measured received powers at a reference distance rather than assuming $R_0^m = R_0^i$ in order to eliminate the effect of antenna gains.

In environments with such uncertainties (e.g. indoor, urban etc) ray-tracing concept can be used to predict the radio wave propagation (Degli-Esposti, Lombardi et al. 1998; Remley, Anderson et al. 2000). Here, the radio waves are considered to follow the properties similar to visual light propagation in the presence of transparent obstacles.

3.3 Power control analysis

(a) Optimum Carrier-to-Interference Ratio

CDMA base stations have a minimum CIR value (γ_{min}) which guarantee QoS reception. In CIR based power control algorithms such as (Foschini and Miljanic 1993; Uykan and Koivo 2004; Uykan and Koivo 2006) etc the controller is trying to maintain the CIR at a fixed value $\gamma_f \geq \gamma_{min}$. In this paper, we introduce a dynamic target CIR value ($\gamma^t \geq \gamma_{min}$) which is the optimal CIR for the number of clients connected with the server at that instance. The CIR, measured at the server, of the communication with the i^{th} client (γ_i) can be defined as follows,

$$\gamma_i = \frac{R_i}{\sum_{j=1, j\neq i}^{n} R_j} \tag{17}$$

where R_i denotes the received power measured at the server, transmitted by the i^{th} client in ``Watts''. Note that the R_i includes the random noise of the measurements as well. The server is said to have a good communication with the i^{th} sensor, if the γ_i is greater than the threshold value γ^t. Then the above can be expressed in the following form (as in (Zander 1992)),

$$\frac{R_i}{\sum_{j=1}^{n} R_j - R_i} \geq \gamma^t. \tag{18}$$

The vector representation of the above is,

$$\left(\frac{1+\gamma^t}{\gamma^t}\right)\overline{R} \geq 1_n \overline{R}\,, \tag{19}$$

where 1_n is the unity matrix and $\left[\overline{R}\right]_i = R_i$. As proposed by Zander in (Zander 1992) we can derive the optimal γ^t value as follows (see Remark 1),

$$\gamma^t = \frac{1}{(n-1)}, \forall n < n_{max}, \tag{20}$$

which results, $R_i = R^t, \forall i = 1 \ldots n$, i.e. the received power values of the signals from every client, measured at the server should be equal. Here R^t is the target received power. This reduces the CIR balancing problem to a simple power control problem as presented in the next section.

Using the Perron-Froebenius theorem (see (Varga 1962)), the largest real eigenvalue of the matrix 1_n can be found as n. Selecting $R^t = R_{min}$ results in maintaining the CIR at the optimal value of $\frac{1}{(n-1)}$ while gaining the maximum energy saving in the network.

(b) Transmission Power Control

In this section, we propose a power control scheme to maintain the variable CIR presented above. Since we proved that maintaining a constant received power at the base station satisfies the optimal CIR condition, the ultimate target of the power control algorithm is to maintain R_m^i at R^t.

(c) Iterative Controller

The iterative power control algorithm is proposed as follows;

$$\dot{P}_i^T = f(R^i - R_m^i)\,. \tag{21}$$

Here the $f(\cdot)$ is defined as any function satisfying the Lipschitz condition,

$$f(|a-b|) \leq k_1 |a-b| \tag{22}$$

where $k_1 \in [0,1]$ is the Lipschitz constant for the function $f(\cdot)$.

Proposition 1: The controller converges the R_m^i, starting from any arbitrary value, to R^t, if the transceiver gains remain constant.

Proof. From the path loss model between the client (15) and the server (16) nodes, we have

$$R_m^i = P_i^T - P_m^T + R_i^m)$$

and since P_m^T is a constant in our problem, the received power at the client node remains a constant. Then the controller becomes,

$$P_i^T = f(R^i - P_i^T + P_m^T - R_i^m) \tag{23}$$

resulting,

$$P_i^T = f(C - P_i^T + \upsilon_i)\,,$$

where $C = R^i + P_m^T - \hat{R}_i^m$ is a constant for the time interval. Here the υ_i is the random noise in the R_i^m, i.e. $\hat{R}_i^m = R_i^m + \upsilon_i$. Let $p = (C - P_i^T)$, then $\dot{p} = -\dot{P}_i^T$. The equation (23) can then be written in the vector form as,

$$\dot{\overline{p}} = -\phi(\overline{p} + \overline{\upsilon}) = \phi(-\overline{p} - \overline{\upsilon}), \quad (24)$$

where $[\overline{p}]_i = P_i^T, [\overline{\upsilon}]_i = \upsilon_i$ and $\phi : \Re^n \rightarrow \Re^n$ i.e. $\phi(\overline{a}) = [f(a_1)\ldots f(a_n)]^T$, $\overline{a} = [a_1 \ldots a_n]^T \in \Re^n$ and $\phi(\overline{a}) = 0$ if $\overline{a} = 0$, thus the equilibrium point is the desired transmit power in (21) giving the optimal CIR in (20). Then as in (Uykan and Koivo 2004), selecting $\overline{a} = -\overline{p}_a - \overline{\upsilon}$ and $\overline{b} = -\overline{p}_b - \overline{\upsilon}$ yields,

$$\| \phi(\overline{p}_a) - \phi(\overline{p}_b) \| \le k_1 \| (\overline{p}_a - \overline{p}_b) \|. \quad (25)$$

Since the above expression satisfies the Lipschitz conditions the system converges toward the desired power vector. (see (Uykan and Koivo 2004) and references there)
The numerical simulation results presented in Fig 6 shows the behavior of two controller functions; (1) A linear controller (f_L), and (2) A sigmoid based controller (f_S), defined as,

$$f_L(a) = 0.3 * a,$$

$$f_S(a) = 2\left(-0.5 + \frac{1}{1 + exp(-a)}\right)$$

Remark: Lipschitz constants of the $f_L(\cdot)$ is 0.3 and that of $f_S(\cdot)$ is 0.5 (see (Uykan and Koivo 2004)) thus the above control functions satisfy the condition in (22) and hence agree with the theoretical proof for convergence.

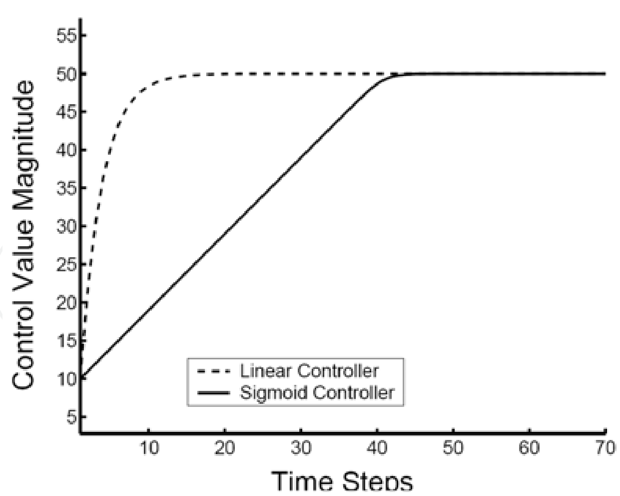

Fig. 6. - Numerical results showing the convergence of the controllers. Here $C = 50$ and $p(0) = 10$

3.4 Experimental Results

In the experimental evaluation we use two controller configurations, (i) Centralized implementation *(see Fig 7(a))* and (ii) Decentralized implementation *(see Fig 7(b))*. For the centralized implementation the server node transmits the signal strength of the received signal back to the client node, which will be used in the power control process. This uses the controller configuration expressed in the equation (21). In the distributed implementation, the client nodes make use of the local signal strength measurement for the power control process. For this approach the second configuration of the power control algorithm expressed by the equation (23) is used.

The experimental evaluation is conducted with the Micaz transceivers (Fig 8) developed by XBow technologies (Crossbow 2007). In Micaz hardware, the transmission power is controlled via an index (see (Chipcon 2004) on mapping of the index to dBm). The experiments were done for two basic cases, (i) static environment where the gains of the communication does not change significantly with in the time interval, and (ii) dynamic environment where the server node randomly moves within it's communication range. We use five cases for each environment to study the performance of the control algorithms. The controller implementation in each client node is shown in the Table 2.

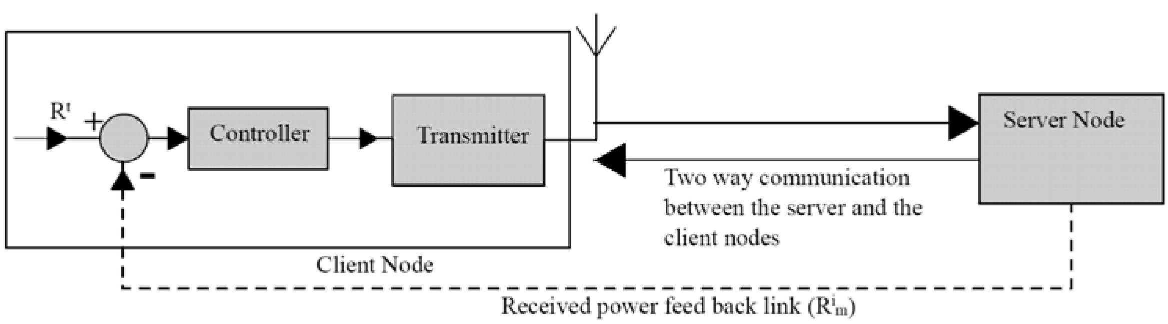

(a) Centralized Implementation of the controller

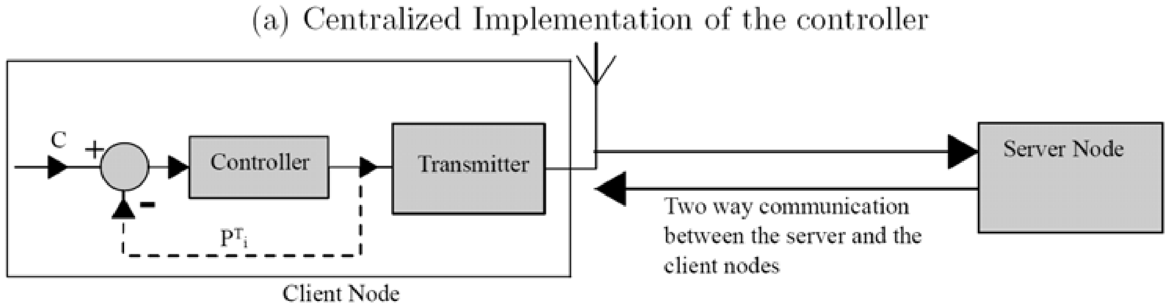

(b) Decentralized Implementation of the controller

Fig. 7. - Controller Configurations

Fig. 8. - Micaz node used for the experiment

(a) Static Environment

For this experiment we choose an environment with no or limited link gain variation (mostly due to the receiver noise). The Fig 9 shows the variation of received power measurements and the transmission power values of the client nodes. For this experiment, the target received power at the server node (R^t) is selected as $-70dBm$. According to the experiment results, the centralized controllers perform an accurate power control than the decentralized ones. Moreover, the centralized controllers demonstrate more robustness to measurement errors comparing with the decentralized one.

Client No.	Control Algorithm/ function
1	Centralized/ f_L
2	Centralized/ f_S
3	De-centralized/ f_L
4	De-centralized/ f_S

Table 2. - Client nodes and their controllers

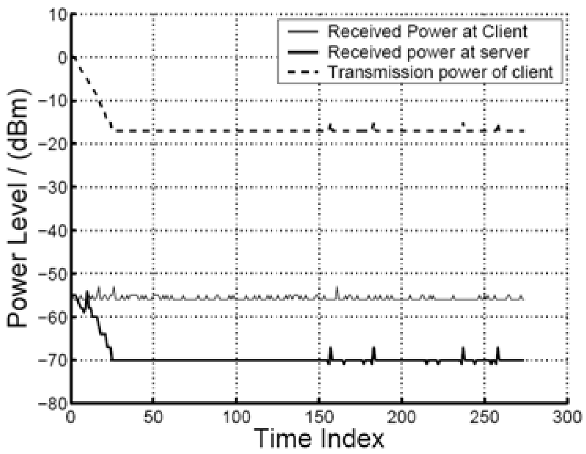

(a) Centralized implementation of the linear controller

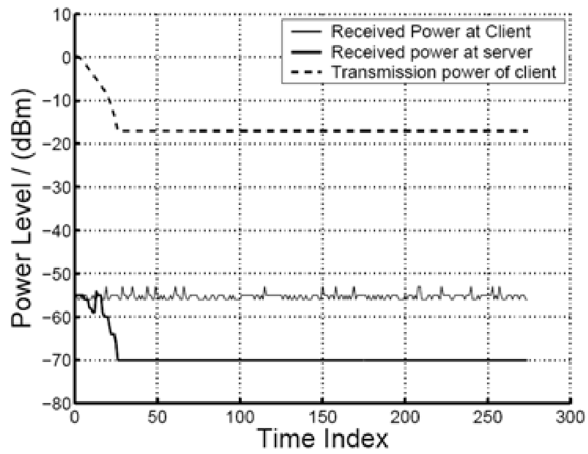

(b) Centralized implementation of the sigmoid controller

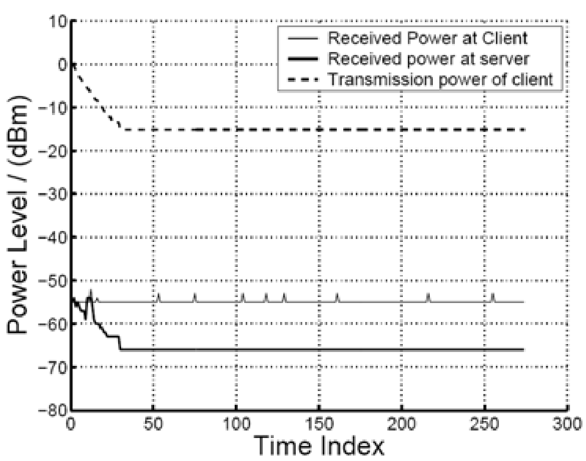

(c) De-centralized implementation of the linear controller

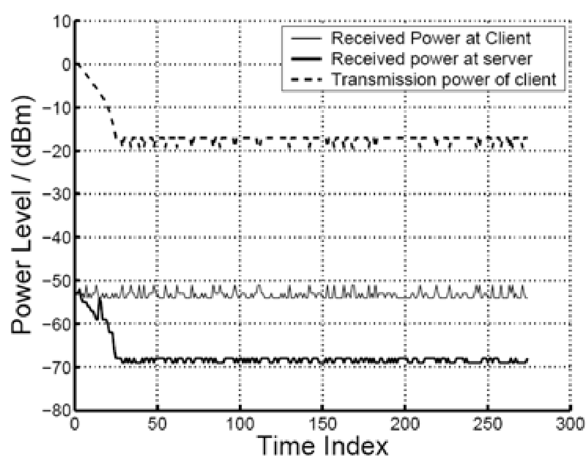

(d) De-centralized implementation of the sigmoid controller

Fig. 9. - Behavior of the iterative controller in a static environment

(b) Dynamic Environment

The Figure 10 shows the variation of received power measurements and the transmission power values of the client nodes. The target received power at the server node (R^t) is selected as $-70dBm$. In a dynamic environment, neither the centralized controllers nor the decentralized controllers perform well in maintaining a constant RSS at the server node. However, the centralized and decentralized implementation of the sigmoid function based controller performed well than the other controller configurations.

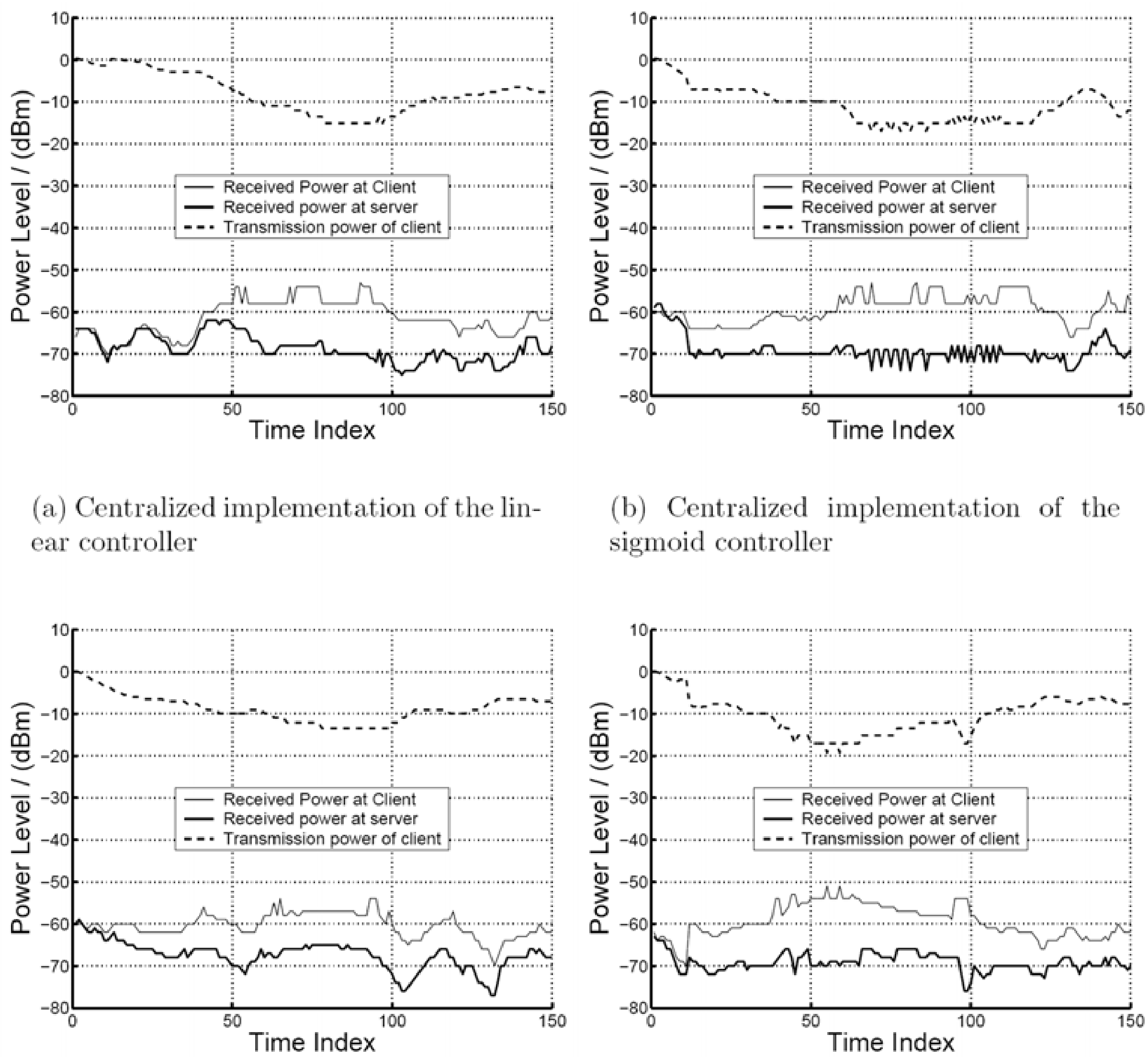

(a) Centralized implementation of the linear controller

(b) Centralized implementation of the sigmoid controller

(c) De-centralized implementation of the linear controller

(d) De-centralized implementation of the sigmoid controller

Fig. 10. - Implementation of the iterative controller in a dynamic environment

4. Conclusion

The first section of this chapter introduces architecture for an all-to-all ad-hoc wireless network that satisfies the QoS requirements as well as power saving aspects. The CDMA based communication in the proposed network enables the operation in a very narrow band as well as maintaining a larger member base. This makes this network extremely suitable for military, swarm robotics and sensor network applications that require larger member base dispersed in relatively close proximity (i.e. within the single hop range of the transmitters) and simultaneous / delay-free communication within the network. The simulation case studies illustrate the behaviour of the controller in ideal conditions. Moreover, the theoretical assertions of network capacity and selection of target RSS value were illustrated.

Moreover, the controller behaviours in dynamic and real-world scenarios are tested using computer simulations.
In the second section of the chapter we introduced a power control algorithm which uses RSS measurements which is facilitated by most commercially available transceivers (in comparison with the CIR measurements presented in (Foschini and Miljanic 1993; Uykan and Koivo 2004) etc,). Since the control scheme focuses on maintaining the least power required for the base station / mobile data collector to capture the data packet, the clients transmit the signal in the minimum possible power which ensures the optimal CIR for every client. This effectively enhances the battery life of the power critical client nodes while maintaining a better quality of service. The experimental results verify the convergence of the power control scheme in a static environment as well as the practical applicability of the proposed controller.

5. References

Agelet, F. A., F. P. Fontan, et al. (1997). "Fast ray tracing for microcellular and indoor environments." Magnetics, IEEE Transactions on 33(2): 1484-1487.

Akyildiz, I. F., E. Ekici, et al. (2003). "A Distributed Multicast Routing Scheme for Multi-Layered Satellite IP Networks." Wireless Networks 9(5): 535-544.

Almeroth, K. C. (2000). "The evolution of multicast: from the MBone to interdomain multicast to Internet2 deployment." Network, IEEE 14(1): 10-20.

Batchelor, A., W. Y. Ochieng, et al. (1996). Design features of D-GNSS reference stations. Satellite Systems for Mobile Communications and Navigation, 1996., Fifth International Conference on.

Cai, M., W. Wang, et al. (2004). Power control algorithm for time-varying CDMA cellular systems. Intelligent Mechatronics and Automation, 2004. Proceedings. 2004 International Conference on.

Chan, Y. S., J. W. Modestino, et al. (2007). "An End-to-End Embedded Approach for Multicast/Broadcast of Scalable Video over Multiuser CDMA Wireless Networks." Multimedia, IEEE Transactions on 9(3): 655-667.

Chen, M.-S., J.-C. Chen, et al. (1996). "On general results for all-to-all broadcast." Parallel and Distributed Systems, IEEE Transactions on 7(4): 363-370.

Chipcon (2004). "C2240 Transceiver Datasheet." Chipcon Systems.

Cooper, G. R. and R. W. Nettleton (1978). "A spread-spectrum technique for high-capacity mobile communications." Vehicular Technology, IEEE Transactions on 27(4): 264-275.

Crossbow (2007). "Crossbow Technologies Incorporated." http://www.xbow.com.

Degli-Esposti, V., G. Lombardi, et al. (1998). "Measurement and ray-tracing prediction of indoor channel parameters." Electronics Letters 34(22): 2167-2168.

ElBatt, T. and A. Ephremides (2004). "Joint scheduling and power control for wireless ad hoc networks." Wireless Communications, IEEE Transactions on 3(1): 74-85.

Ellersick, F. (1984). "A conversation with Claude Shannon." Communications Magazine, IEEE 22(5): 123-126.

Erceg, V., L. J. Greenstein, et al. (1999). "An empirically based path loss model for wireless channels in suburban environments." Selected Areas in Communications, IEEE Journal on 17(7): 1205-1211.

Foschini, G. J. and Z. Miljanic (1993). "A simple distributed autonomous power control algorithm and its convergence." Vehicular Technology, IEEE Transactions on 42(4): 641-646.

Gilhousen, K. S., I. M. Jacobs, et al. (1991). "On the capacity of a cellular CDMA system." Vehicular Technology, IEEE Transactions on 40(2): 303-312.

Gomez, J. and A. T. Campbell (2007). "Variable-Range Transmission Power Control in Wireless Ad Hoc Networks." Mobile Computing, IEEE Transactions on 6(1): 87-99.

Grandhi, S. A., R. Vijayan, et al. (1994). "Distributed power control in cellular radio systems." Communications, IEEE Transactions on 42(234): 226-228.

Grandhi, S. A., R. Vijayan, et al. (1993). "Centralized power control in cellular radio systems." Vehicular Technology, IEEE Transactions on 42(4): 466-468.

Grandhi, S. A., R. D. Yates, et al. (1997). "Resource allocation for cellular radio systems." Vehicular Technology, IEEE Transactions on 46(3): 581-587.

Guo, S. and O. Yang (2006). "A Constraint Formulation for Minimum-Energy Multicast Routing in Wireless Multihop Ad-hoc Networks." Wireless Networks 12(1): 23-32.

Hou, Y. T., Y. Shi, et al. (2006). "Maximizing the Lifetime of Wireless Sensor Networks through Optimal Single-Session Flow Routing." Mobile Computing, IEEE Transactions on 5(9): 1255-1266.

Klein, T. E. and H. Viswanathan (2006). "Centralized power control and routing policies for multihop wireless networks." Information Theory, IEEE Transactions on 52(3): 849-866.

Knisely, D. N., S. Kumar, et al. (1998). "Evolution of wireless data services: IS-95 to cdma2000." Communications Magazine, IEEE 36(10): 140-149.

Lim, S., K. M. K. H. Leong, et al. (2005). "Adaptive power controllable retrodirective array system for wireless sensor server applications." Microwave Theory and Techniques, IEEE Transactions on 53(12): 3735-3743.

Lin, S., J. Zhang, et al. (2006). ATPC: adaptive transmission power control for wireless sensor networks. Proceedings of the 4th international conference on Embedded networked sensor systems. Boulder, Colorado, USA, ACM Press: 223-236.

Prasad, R. and T. Ojanpera (1998). A survey on CDMA: evolution towards wideband CDMA. Spread Spectrum Techniques and Applications, 1998. Proceedings., 1998 IEEE 5th International Symposium on.

Puccinelli, D. and M. Haenggi (2006). Multipath fading in wireless sensor networks: measurements and interpretation. Proceeding of the 2006 international conference on Communications and mobile computing. Vancouver, British Columbia, Canada, ACM Press: 1039-1044.

Remley, K. A., H. R. Anderson, et al. (2000). "Improving the accuracy of ray-tracing techniques for indoor propagation modeling." Vehicular Technology, IEEE Transactions on 49(6): 2350-2358.

Santos, R. A., O. Alvarez, et al. (2005). Experimental analysis of wireless propagation models with mobile computing applications. Electrical and Electronics Engineering, 2005 2nd International Conference on.

Sato, R., H. Sato, et al. (2005). A SBR estimation for indoor wave propagation through dielectric walls. Antennas and Propagation Society International Symposium, 2005 IEEE.

Schiller, J. (2003). Mobile Communications, Addison-Wesley.

Scholtz, R. A. (1994). The evolution of spread-spectrum multiple-access communications. Spread Spectrum Techniques and Applications, 1994. IEEE ISSSTA '94., IEEE Third International Symposium on.

Tam, W. K. and V. N. Tran (1995). "Propagation modelling for indoor wireless communication." Electronics & Communication Engineering Journal 7(5): 221-228.

Transier, M., H. Fubler, et al. (2007). "A hierarchical approach to position-based multicast for mobile ad-hoc networks." Wireless Networks 13(4): 447-460.

Uykan, Z. and H. N. Koivo (2004). "Sigmoid-basis nonlinear power-control algorithm for mobile radio systems." Vehicular Technology, IEEE Transactions on 53(1): 265-270.

Uykan, Z. and H. N. Koivo (2006). "Proportional power control algorithm for time varying link gains in cellular radio systems." Vehicular Technology, IEEE Transactions on 55(1): 341-349.

Varga, R. S. (1962). Matrix Iterative Analysis. N.J., Prentis Hall, Inc.

Yang, L.-L. (2006). "MIMO-assisted space-code-division multiple-access: linear detectors and performance over multipath fading channels." Selected Areas in Communications, IEEE Journal on 24(1): 121-131.

Yang, Y. and J. Wang (1998). "On blocking probability of multicast networks." Communications, IEEE Transactions on 46(7): 957-968.

Yang, Y. and J. Wang (2001). "Pipelined all-to-all broadcast in all-port meshes and tori." Transactions on Computers 50(10): 1020-1032.

Zander, J. (1992). "Performance of optimum transmitter power control in cellular radio systems." Vehicular Technology, IEEE Transactions on 41(1): 57-62.

Mobile and Wireless Communications Network Layer and Circuit Level Design

Edited by Salma Ait Fares and Fumiyuki Adachi

ISBN 978-953-307-042-1
Hard cover, 404 pages
Publisher InTech
Published online 01, January, 2010
Published in print edition January, 2010

Mobile and wireless communications applications have a clear impact on improving the humanity wellbeing. From cell phones to wireless internet to home and office devices, most of the applications are converted from wired into wireless communication. Smart and advanced wireless communication environments represent the future technology and evolutionary development step in homes, hospitals, industrial, vehicular and transportation systems. A very appealing research area in these environments has been the wireless ad hoc, sensor and mesh networks. These networks rely on ultra low powered processing nodes that sense surrounding environment temperature, pressure, humidity, motion or chemical hazards, etc. Moreover, the radio frequency (RF) transceiver nodes of such networks require the design of transmitter and receiver equipped with high performance building blocks including antennas, power and low noise amplifiers, mixers and voltage controlled oscillators. Nowadays, the researchers are facing several challenges to design such building blocks while complying with ultra low power consumption, small area and high performance constraints. CMOS technology represents an excellent candidate to facilitate the integration of the whole transceiver on a single chip. However, several challenges have to be tackled while designing and using nanoscale CMOS technologies and require innovative idea from researchers and circuits designers. While major researchers and applications have been focusing on RF wireless communication, optical wireless communication based system has started to draw some attention from researchers for a terrestrial system as well as for aerial and satellite terminals. This renewed interested in optical wireless communications is driven by several advantages such as no licensing requirements policy, no RF radiation hazards, and no need to dig up roads besides its large bandwidth and low power consumption. This second part of the book, Mobile and Wireless Communications: Key Technologies and Future Applications, covers the recent development in ad hoc and sensor networks, the implementation of state of the art of wireless transceivers building blocks and recent development on optical wireless communication systems. We hope that this book will be useful for students, researchers and practitioners in their research studies.

InTech Europe
University Campus STeP Ri
Slavka Krautzeka 83/A
51000 Rijeka, Croatia
Phone: +385 (51) 770 447
Fax: +385 (51) 686 166
www.intechopen.com

InTech China
Unit 405, Office Block, Hotel Equatorial Shanghai
No.65, Yan An Road (West), Shanghai, 200040, China
中国上海市延安西路65号上海国际贵都大饭店办公楼405单元
Phone: +86-21-62489820
Fax: +86-21-62489821